

PACS numbers: 61.43.Gt, 61.72.Mm, 64.70.dg, 68.35.Ct, 81.05.Bx, 81.05.Ni, 81.30.Fb

The Effect of Reinforcement on the Microstructure of High-Carbon Steel Castings

Ye. H. Aftandilyants, V. A. Slyusarev, Yu. H. Kvasnyts'ka,
I. A. Shalevs'ka, P. B. Kalyuzhnyy, V. I. Veys, T. V. Stepanova,
and Zh. V. Parkhomchuk

*Physico-Technological Institute of Metals and Alloys, N. A. S. of Ukraine,
34/1 Academician Vernadsky Blvd.,
UA-03142 Kyiv, Ukraine*

This article presents the results of a study on the effect of reinforcement on the microstructure of high-carbon steel castings. Plates with thicknesses of 0.5, 1.0, 1.5, and 3.0 mm are used as reinforcing elements. The implantation of the inserts into the castings is carried out by placing them into a pre-formed cavity in a polystyrene-foam model, which is then set into a mould and poured with molten high-carbon steel. Examination of the ‘insert–matrix’ interfaces revealed both defect-free and defective contact areas, the latter appearing as gaps with maximum widths exceeding 100 μm . A correlation is established between the heating temperature of the inserts and the length of the gap-containing interface. A quantitative relationship is determined between the insert thickness and the extent of the gap in the ‘reinforcing element–matrix’ contact zone, and a mechanism of this effect is proposed. The influence of insert thickness on the minimum, maximum, and average pearlite-grain area, as well as on its distribution within the matrix of the castings, is analysed. Analytical models are developed to describe the effect of insert thickness and gap length on the average pearlite-grain area in the microstructure of the casting near the insert surface and at a distance of 20 mm from it. As found, the minimum average pearlite-grain area near the

Corresponding author: Yevhen Hryhorovych Aftandilyants
E-mail: aftyev@yahoo.com

Citation: Ye. H. Aftandilyants, V. A. Slyusarev, Yu. H. Kvasnyts'ka, I. A. Shalevs'ka, P. B. Kalyuzhnyy, V. I. Veys, T. V. Stepanova, and Zh. V. Parkhomchuk, The Effect of Reinforcement on the Microstructure of High-Carbon Steel Castings, *Metallofiz. Noveishie Tekhnol.*, 48, No. 2: 153–168 (2026). DOI: [10.15407/mfint.48.02.0153](https://doi.org/10.15407/mfint.48.02.0153)

© Publisher PH “Akademperiodyka” of the NAS of Ukraine, 2026. This is an open access article under the CC BY-ND license (<https://creativecommons.org/licenses/by-nd/4.0>)

insert surface reaches $170.4 \mu\text{m}^2$ at an insert thickness of 2.2 mm and $148.2 \mu\text{m}^2$ at a distance of 20 mm for a 2.0 mm thick insert, which is 6 and 14 times lower, respectively, than in castings without inserts. The most pronounced grain-refinement effect is observed for inserts with a thickness of 2.0–2.2 mm and a gap length at the ‘insert–matrix’ interface in the range of 62–72%.

Key words: steel, reinforcement, structure, casting, pearlite, solidification.

В статті описано результати дослідження впливу армування на мікроструктуру виливків з високовуглецевої криці. Як армувальні елементи використовували пластини товщиною у 0,5, 1,0, 1,5, 3 мм. Імплантацію армувальних вставок у виливки виконували шляхом введення їх у попередньо підготовлену порожнину в пінополістироловий модель, що встановлювався у ливарну форму та заливався рідкою високовуглецевою крицею. За результатом дослідження меж поділу між вставками та матричним стопом встановлено, що є як бездефектні, так і дефектні місця контактів у вигляді зазорів, в яких максимальна висота зазору може бути понад 100 мкм. Встановлено кореляцію між температурою нагрівання вставок і довжиною зони контакту із зазором і визначено кількісну закономірність впливу товщини вставок на протяжність зазору в зоні контакту «армувальний елемент–матриця» та запропоновано механізм впливу. Показано вплив товщини вставок на мінімальну, максимальну та середню площу зерен перліту та розподіл їх у матриці виливків. Встановлено аналітичні залежності впливу товщини вставок і довжини зазору на середню площу зерен перліту мікроструктури виливків біля поверхні вставок і на віддалі 20 мм від них. Визначено, що мінімальне значення середньої площі зерна перліту біля поверхні вставок сягає $170,4 \mu\text{m}^2$ за товщини вставки у 2,2 мм і $148,2 \mu\text{m}^2$ на віддалі у 20 мм за товщини вставки у 2,0 мм, що в 6 і 14 разів відповідно менше, ніж у виливках без вставок. За результатами дослідження встановлено, що найбільш ефективний вплив армувальних вставок на диспергування перлітної структури спостерігається за їхньої товщині від 2,0 до 2,2 мм і довжині зазору на межі поділу «вставка–матриця» від 62 до 72%.

Ключові слова: криця, армування, структура, виливок, перліт, тверднення.

(Received 17 July, 2025; in final version, 15 October, 2025)

1. INTRODUCTION

Reinforcement of castings is one of the effective methods for improving the quality and manufacturability of components with complex geometry. As a technological approach, reinforcement enables the combination of several ferrous materials with different physical properties within a single casting, while maintaining relatively low production costs through casting processes. For example, a grey cast iron matrix can be reinforced with a high-carbon steel insert in areas requiring in-

creased hardness. Alternatively, stainless steel inserts may be used in zones where localized corrosion resistance is needed. Another case involves using a hard matrix made of high-carbon alloy steel and a softer steel insert to facilitate machining in specific locations, such as for threading in screw joints—either without additional machining or with only minimal post-processing.

Reinforced castings are produced by various methods of liquid-phase bonding, which involve the consolidation of solid reinforcing elements with molten metal that, upon solidification, forms a composite. The structure and properties of reinforced castings are determined by the combination of the structure and properties of the reinforcing elements, the matrix, and their interfacial region.

During pouring, cooling, and solidification, physical and chemical interactions occur between the reinforcing elements and the matrix. These interactions lead to changes in the physical, chemical, and structural homogeneity of the matrix and contribute to the formation of the interface between the reinforcing element and the matrix.

The heat balance equation during the solidification of a metal layer on a solid reinforcing element is as follows:

$$dq_{\text{mould}} = dq_{\text{cool}} + dq_{\text{cryst}} + dq_{\text{reinf}}. \quad (1)$$

Here, dq_{mould} —heat removed to the mould from the solidified metal, dq_{cool} —heat released during cooling of the melt from the pouring temperature to the solidification temperature, dq_{cryst} —heat released during metal crystallization, dq_{reinf} —heat released during cooling of the metal from the crystallization temperature to the temperature of the solid reinforcing element.

The reinforcing element accumulates part of the heat released during melt solidification, which promotes accelerated crystallization and suppresses segregation processes. In this case, the intensity of internal heat removal can be 3 to 5 times higher than that of external heat dissipation through the mould wall [1].

The amount of heat transferred under steady-state heat exchange conditions from the volume of liquid metal to the surface of the reinforcing element dq_{reinf} is determined by the following equation [1]:

$$q_{\text{reinf}} = \beta(t_1 - t_s)\tau. \quad (2)$$

Here, β —contact heat transfer coefficient from the liquid metal to the surface of the reinforcing element, t_1 and t_s —temperature of the melt and the initial temperature of the surface of the reinforcing element, respectively, τ —duration of heat exchange.

According to [2], the heating temperature of a metallic component (t_{heat}) in an external environment with temperature (t_{env}) is determined

by the following expression:

$$t_{\text{heat}} = (t_{\text{env}} - t_{\text{init}}) \left(1 - e^{-\frac{\alpha F \tau}{mc}} \right) + t_{\text{init}} \frac{\partial^2 \Omega}{\partial v^2}. \quad (3)$$

Here, t_{init} —initial temperature of the metallic component, m and F —mass and surface area of the metallic component, respectively, c —heat capacity of the metal, α —heat transfer coefficient of the metal, τ —duration of heat exchange.

The interaction between the reinforcing element and the solidifying melt occurs in two stages. The first stage begins filling during mould and is accompanied by the formation of a solidified metal layer on the surface of the insert. At this stage, the most intense heat exchange takes place during the initial period of layer formation. A study of the solidification dynamics of the melt on the reinforcing element [3] revealed that the contact between the outer surface of the insert and the solidifying melt is discrete in nature.

The condition of the contact between the melt and the surface of the insert has a significant effect on the intensity of heat exchange with the reinforcing element. In the contact zone, oxide films and gas layers are formed, which introduce considerable thermal resistance to the heat transfer from the solidifying melt to the reinforcing element and contribute to the formation of a gap.

The formation of a gap between the reinforcing element and the matrix occurs during the heating of the insert to a temperature below the solidus point, as well as due to gas release at the surface of the reinforcing element caused by decarburization and moisture evaporation. During the interaction of the reinforcing element with the melt, gases trapped in surface depressions and roughness zones heat up and expand, disrupting the metal solidified on the surface of the insert [4, 5].

The second stage involves the remelting of the solidified layer. During the solidification of a reinforced casting or ingot, these stages are repeated multiple times.

According to [1], the introduction of 0.6–0.9% of a solid insert into a mould measuring 250×1650 mm results in its complete dissolution and a 60% reduction in the columnar crystal zone. The addition of 1.5–2.0% of the solid phase enables ingot reinforcement and completely eliminates the columnar zone. This leads to a reduction in axial segregation, an increase in impact toughness, and an improvement in the macrostructure of the cast metal.

A study of the thermophysical conditions of reinforced melt cooling during continuous steel casting [6] showed that the most effective cooling occurs when 1.5% of the solid phase is introduced in the form of a steel strip 0.4 m wide and 0.0015 m thick. In this case, the greatest portion of heat is consumed for the remelting of the initially solidified

layer.

The change in the degree of superheat removed during the solidification-on-insert process is shown in Fig. 1.

The consolidation of reinforcing inserts placed in the mould with the solidifying melt after pouring occurs through the formation of a contact zone, which is driven by mechanical and adhesion forces, as well as diffusion processes [7].

Mechanical bonding is formed when the melt does not wet the surface of the solid element and no chemical interaction occurs between them. During the shrinkage of the solidifying melt, normal pressure is exerted on the reinforcing insert, which ensures mechanical bonding. This pressure is directly proportional to the shrinkage magnitude, the elastic modulus, and the Poisson's ratio of both the insert and the matrix, and inversely proportional to the contact surface area of the insert [7].

The level of mechanical bonding is characterized by the coefficient of friction between the solid element and the solidified casting, which can be increased by creating grooves or notches on the surface of the reinforcing inserts. Mechanical bonding is effective under static loading. However, a gap may form between the solid element and the cast metal due to the incomplete filling of surface depressions, especially when the melt poorly wets the solid surface. Therefore, surface notches enhance mechanical bonding but also contribute to the formation of intermittent gaps, which are undesirable under cyclic loading and vibrations.

The pressure, at which the liquid metal comes into contact with the

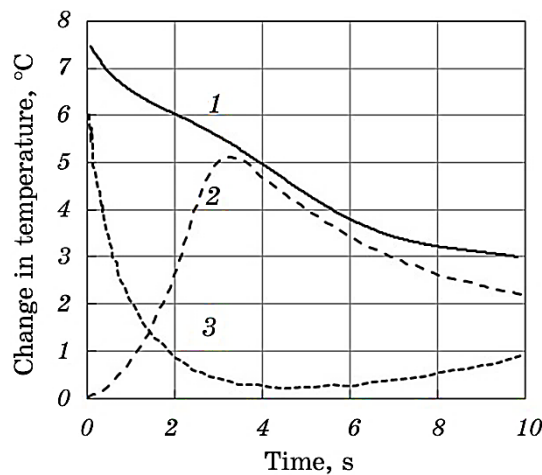


Fig. 1. Cooling of liquid steel by the reinforcing insert (3), heating and remelting of the solidified layer (2), and total cooling of the melt (1) [1].

solid element, influences the formation of mechanical bonds. Higher pressure improves the filling of surface irregularities and reduces the likelihood of forming intermittent gaps.

In the case of laminar melt flow and insufficient wetting of the reinforcing insert surface, the flow takes the form of a rolling wave, and air pockets form between the flow and the solid surface. These air layers contribute to gap formation and weaken the mechanical bond.

The formation of adhesion bonds between the elements of composite castings occurs when the surface of the reinforcing insert is wetted by the melt. Wettability can be controlled by introducing surface-active elements into the melt.

It has been established [7] that increasing the solubility of oxygen, carbon, and boron in the melt improves the wettability of reinforcing elements. For melts that wet oxides, effective surface-active components are those with a high affinity for oxygen or for the metal present in the wetted oxide. In the case of carbides and graphite, surface-active components include carbide-forming elements.

Wettability is enhanced by laminar melt flow during mould filling, increased melt temperature, the use of fluxes, alloying, and increasing the surface roughness of the solid phase.

The formation of diffusion bonding zones occurs when the amplitude of surface atom vibrations in the reinforcing element and the matrix exceeds the gap between them. This process is facilitated by pressing of the reinforcing element against the matrix, increased temperature, and wetting of the solid reinforcing surface by the molten metal.

The strength of diffusion bonds is nearly equal to that of the matrix, whereas the strength of adhesive bonds does not exceed half of the matrix strength.

The refinement of the casting structure upon the introduction of reinforcing elements is associated with a change in the solidification rate of the molten metal, which is characterized by the solidification coefficient.

The solidification coefficient (K) at the 'solid reinforcing element–melt' interface is determined by the following equation [8]:

$$K = \frac{2\lambda(t_{cr} - t_{ae})}{\sqrt{C_l\rho_l(t_p - t_{cr}) + \rho_l L + 0.5C_s\rho_s(t_{cr} - t_{ae})}}. \quad (4)$$

Here, λ —thermal conductivity at the 'reinforcing element–matrix' interface, $J/(cm \cdot s \cdot ^\circ C)$; ρ_s , ρ_l —density of the solid and liquid metal, respectively, g/cm^3 ; C_l , C_s —heat capacity of the liquid and solid metal, $J/(g \cdot ^\circ C)$; t_p , t_{cr} , t_{ae} —pouring temperature, crystallization temperature, and temperature of the reinforcing element, respectively, $^\circ C$; L —latent heat of crystallization, J/g .

Analysis of Eq. (4) shows that the solidification rate of the melt de-

depends on the properties of both the liquid and solid metal, as well as on the temperature of the reinforcing element and the thermal conductivity of the 'reinforcing element–matrix' interface.

According to Ref. [8], when steel chill moulds are heated from 30 to 900°C, the solidification coefficient of cast iron decreases by a factor of 16, and when heated to 1150°C, it decreases by a factor of 4.6.

A review of the literature indicates that reinforcement of castings creates prerequisites for improving their quality. However, the effectiveness of reinforcement strongly depends on the conditions under which the 'reinforcing element–matrix' interface is formed and the development of a gap within this zone, which remains insufficiently studied.

The aim of this study is to investigate the effect of reinforcement on gap formation in the 'reinforcing element–matrix' contact zone and on the microstructure of high-carbon steel castings.

2. EXPERIMENTAL/THEORETICAL DETAILS

Plates with a thicknesses of 0.5, 1.0, 1.5, and 3.0 mm were used as reinforcing elements, with corresponding masses of 1.8, 3.5, 5.3, and 10.6 g. Inserts 0.5 mm thick were made from plates of carbon steel (C = 0.3 wt.%), 1.0 mm thick—from notched carbon steel plates (C = 1.5 wt.%), 1.5 mm—from toothed carbon steel plates (C = 0.6 wt.%), and 3.0 mm—from plates of austenitic stainless steel.

The implantation of reinforcing inserts into the castings was carried out by placing them into preformed cavities in polystyrene foam patterns, which were then positioned in the mould and poured with liquid steel, following the procedure described in [9].

Castings in the form of hollow cylinders with a wall thickness of 7.5 mm were produced by pouring steel melt into expendable pattern moulds containing the pre-installed plates.

The chemical composition of the steel smelted in the induction crucible furnace was as follows (wt.%): C = 0.88, Si = 1.14, Mn = 1.87, Al = 0.076, P = 0.025, S = 0.015. The liquidus temperature of the steel was 1466°C, and the solidus temperature was 1436°C.

Photographs of the areas with inserts implanted into the casting are shown in Fig. 2.

The microstructure of the castings with inserts after solidification was examined using an epi-tip microscope at magnifications of 100×, 200×, and 400×.

The analysis focused on the microstructure of the near-surface zone of the casting at the contact with the insert and at a distance of 20 mm from its boundary.

The effect of the reinforcing inserts on the gap size between the insert and the matrix, as well as on the microstructure of the casting,

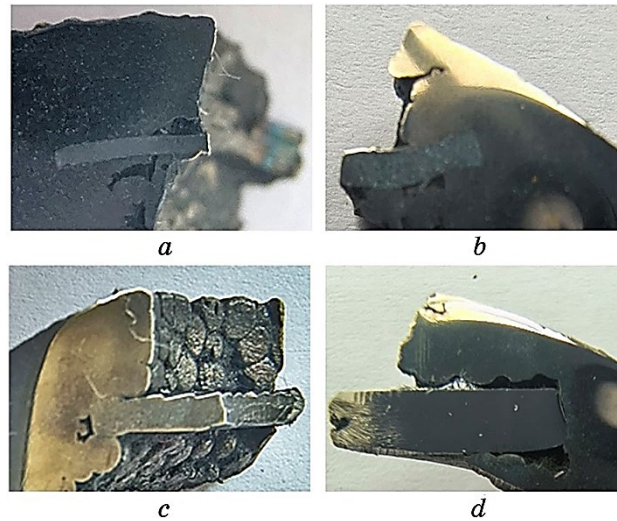


Fig. 2. Sections of castings with inserts of 0.5 mm (a), 1.0 mm (b), 1.5 mm (c), and 3.0 mm (d) thickness.

was assessed using the image analysis software 'ImageJ'.

The effectiveness of the reinforcing inserts on the microstructure of the matrix was evaluated based on the pearlite grain area. During mathematical processing of the obtained results, the minimum, maximum, and average pearlite-grain areas were determined. Histograms of pearlite area distribution by fractions were constructed using the 'Analysis ToolPak' add-in in Microsoft Excel.

Regression and correlation coefficients (R_i) as well as the relative approximation error (δ) were determined with 95% confidence according to the methodology described in [10].

3. RESULTS AND DISCUSSION

The examination of the interfaces between the inserts and the matrix revealed the presence of both nearly defect-free contact zones (Fig. 3, a, b) and zones with gaps of varying size: up to 10 μm (Fig. 3, c), from 10 μm to 100 μm (Fig. 3, d), and over 100 μm (Fig. 3, e).

The analysis showed that, for contact boundary lengths ranging from 3750 μm to 12450 μm , an increase in insert thickness from 0.5 to 3.0 mm leads to a decrease in the length of defect-free contact zones from 88% to 2.0%, while the length of defective zones increases correspondingly from 12% to 98% (Fig. 4, line 1).

The relationship between the insert thickness (δ_i , mm) and the gap

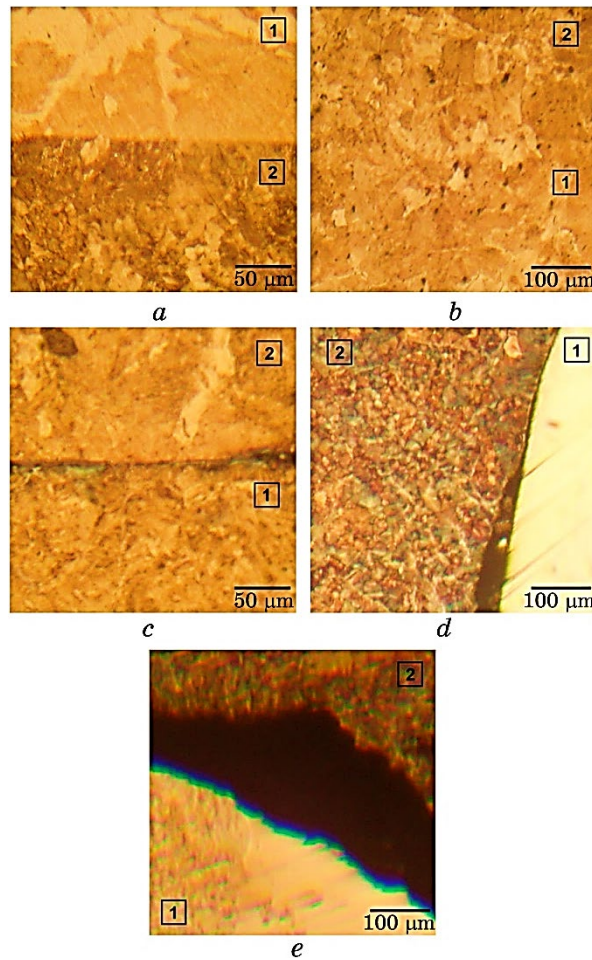


Fig. 3. Microstructure of the contact zones between inserts (1) of 0.5 mm (a), 1.0 mm (b), 1.5 mm (c), and 3.0 mm (d, e) thickness and the matrix (2). Defect-free contact zones (a); gap up to 10 μm (c); gap from 10 to 100 μm (d); gap over 100 μm (e).

length in the ‘reinforcing element–matrix’ contact zone ($l, \%$) is expressed as follows:

$$l = 33.64\delta_i, R = 0.949. \quad (5)$$

To determine the mechanism by which insert thickness influences gap formation, the effect of inserts on the solidification rate of a 7.5 mm thick casting wall was investigated. Based on experimental data from Ref. [11], the influence of the ratio of insert thickness (δ_i, mm)

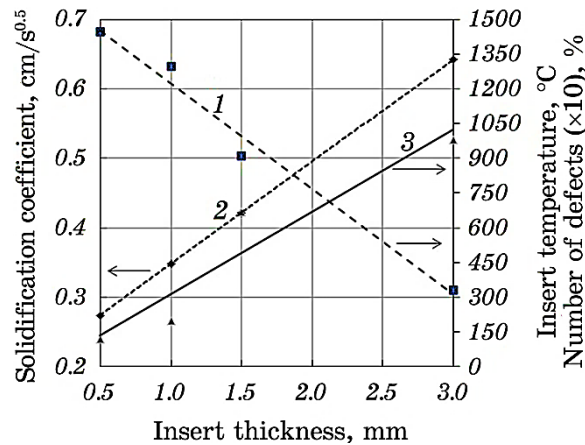


Fig. 4. Effect of insert thickness on the number of defects in the contact zone with the matrix (1), solidification coefficient (2), and insert heating temperature (3) during casting solidification.

to casting-wall thickness (δ_s , mm) on the solidification coefficient (K , $\text{cm}/\text{s}^{0.5}$) was determined and expressed as follows:

$$K = 0.2006 + 0.1105 \delta_i / \delta_s, R = 0.890. \quad (6)$$

Analysis of Eq. (6) shows that the solidification coefficient of the casting wall increases from $0.274 \text{ cm}/\text{s}^{0.5}$ to $0.643 \text{ cm}/\text{s}^{0.5}$ with the use of inserts 0.5 mm and 3.0 mm thick, respectively (Fig. 4, line 2).

Assuming that the main heating of the inserts occurs during the solidification interval of steel, and using the solidification coefficient to determine the solidification time of the casting wall, the insert heating temperature (t_{ins}) was calculated based on Eq. (3) (Fig. 4, line 3).

Correlation analysis showed that there is a statistically significant inverse linear relationship between the insert heating temperature (t_{ins}) and the length of the contact zone with a gap (l , %), expressed as follows:

$$l = 128.98 - 0.0801 t_{\text{ins}}, R = 0.982. \quad (7)$$

This indicates that as the insert temperature increases, the quality of the contact between the reinforcing insert and the matrix improves, reaching a maximum when the insert is heated to the solidification temperature. This is due to surface remelting of the insert and the formation of a diffusion bond with the casting.

The microstructure of the near-surface zone of the casting at the contact with the insert is shown in Fig. 5, and at a distance of 20 mm from it—in Fig. 6.

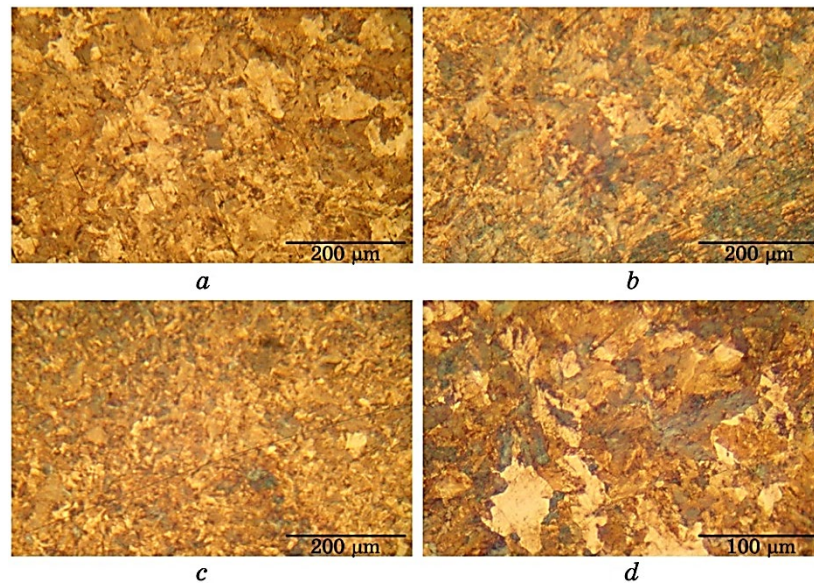


Fig. 5. Microstructure of the near-surface zone of the casting at the contact with the reinforcing insert: insert thickness 0.5 mm (*a*), 1.0 mm (*b*), 1.5 mm (*c*), 3.0 mm (*d*).

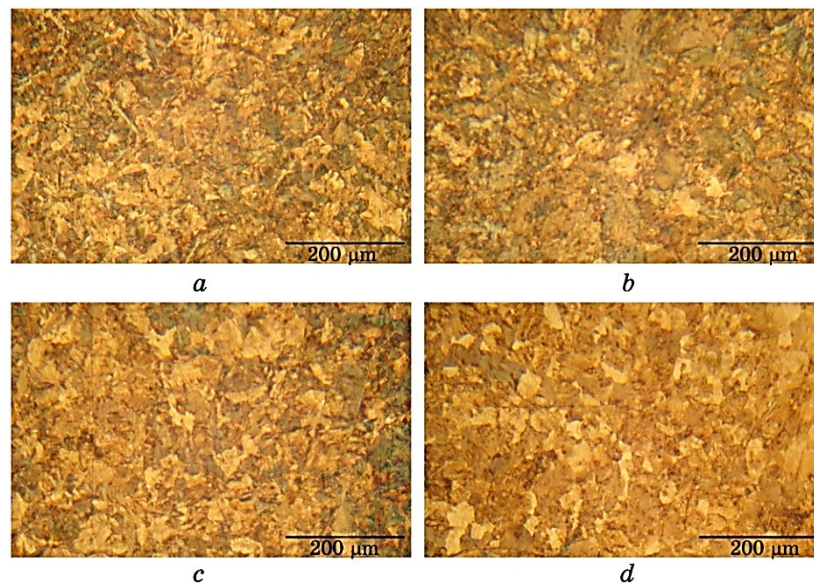
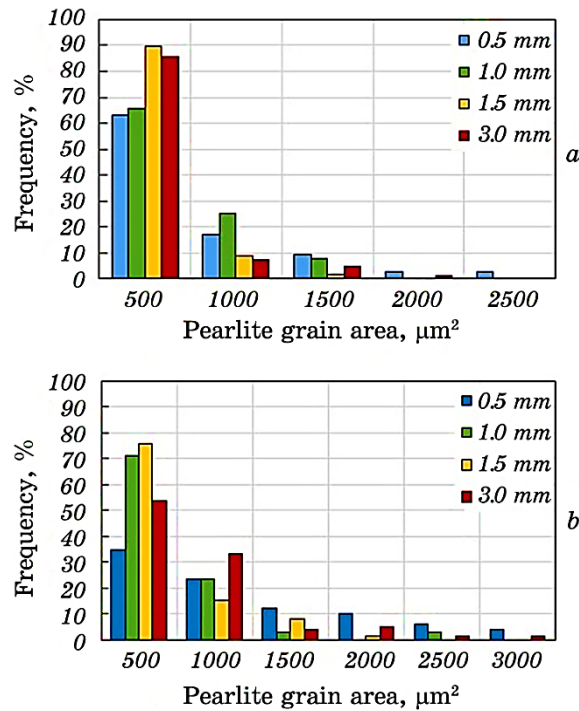


Fig. 6. Microstructure of the near-surface zone of the casting at a distance of 20 mm from the reinforcing insert: insert thickness 0.5 mm (*a*), 1.0 mm (*b*), 1.5 mm (*c*), 3.0 mm (*d*).

TABLE 1. Results of quantitative analysis of the microstructure in the near-surface zone of the casting.

| Insert thickness, mm | Parameter | Pearlite-grain area (S_{per}), μm^2 | |
|----------------------|-----------|----------------------------------------------------|----------------------------------------|
| | | Near the insert | At a distance of 20 mm from the insert |
| 0.5 | Minimum | 64.5 | 57.1 |
| | Maximum | 3861.3 | 8051.0 |
| | Average | 699.3 | 1286.9 |
| 1.0 | Minimum | 66.3 | 68.4 |
| | Maximum | 2933.7 | 2288.7 |
| | Average | 460.1 | 450.9 |
| 1.5 | Minimum | 24.4 | 37.3 |
| | Maximum | 1135.6 | 1995.9 |
| | Average | 249.3 | 382.9 |
| 3.0 | Minimum | 15.8 | 34.1 |
| | Maximum | 2706.6 | 3553.6 |
| | Average | 286.2 | 609.9 |

**Fig. 7.** Distribution of pearlite grain areas in the microstructure of the near-surface zone of the casting at the contact with the insert (*a*) and at a distance of 20 mm from it (*b*).

The results of the quantitative analysis of the microstructure in the near-surface zone of the casting at the contact with the insert and at a distance of 20 mm from it are presented in Table 1, and the distribution of pearlite grain areas by size is shown in Fig. 7.

The data in Table 1 show that the minimum pearlite grain area in the microstructure near the insert surface ranges from $15.8 \mu\text{m}^2$ to $66.3 \mu\text{m}^2$, while the maximum values range from $1135.6 \mu\text{m}^2$ to $3861.3 \mu\text{m}^2$. The corresponding values at a distance of 20 mm from the inserts are $34.1 \mu\text{m}^2$ to $68.4 \mu\text{m}^2$ for the minimum and $1995.9 \mu\text{m}^2$ to $8051.0 \mu\text{m}^2$ for the maximum grain area. This means that near the insert surface, the minimum pearlite grain area is 3–216% smaller, and the maximum is 78–208% smaller compared to the values at a distance of 20 mm.

At the same time, an increased number of fine pearlite grains are observed in the microstructure of the castings near the insert surface. For example, 63% to 90% of pearlite grains have an area ranging from $500 \mu\text{m}^2$ to $1000 \mu\text{m}^2$, which are 19% to 82% higher than at a distance of 20 mm from the inserts (Fig. 7).

The effect of insert thickness (δ , mm) on the average pearlite grain area (S_{avp} , μm^2) is shown in Fig. 8, *a*. It can be seen that both near the insert surface and at a distance of 20 mm, the inserts exhibit an extreme (nonlinear) effect on the average grain area.

This is because, during pouring of the melt into the mould containing the reinforcing insert, the interaction between the insert and the matrix is accompanied by heating of the insert and the formation of a gap between the insert and the matrix. An increase in insert temperature promotes the formation of a strong diffusion bond, but at the

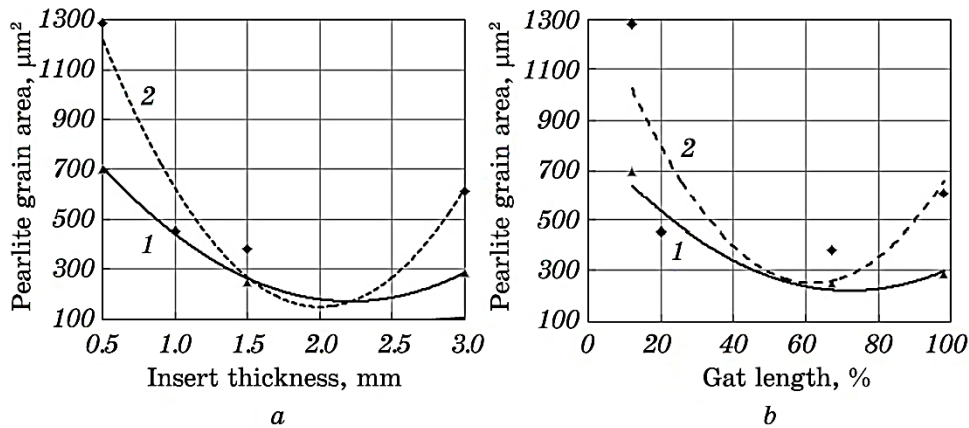


Fig. 8. Effect of insert thickness (*a*) and gap length (*b*) on the average pearlite-grain area in the microstructure of the casting near the insert surface (*1*) and at a distance of 20 mm (*2*).

same time reduces the solidification rate of the melt near the insert, which leads to coarsening of the structural grains.

The formation of a gap between the insert and the matrix reduces heat transfer at the interface, as the thermal conductivity of air is 700–800 times lower than that of steel. This creates conditions that slow down the heating of the reinforcing element and, as a result, accelerate the solidification rate and promote structural refinement.

For the microstructure of the casting near the insert surface and at a distance of 20 mm from it, the pattern of this extreme effect is expressed as follows (Fig. 8, *b*).

In the near-surface layer of the casting, directly in the contact zone with the inserts, the dependence of the average pearlite-grain area on insert thickness is described by the following regression equation:

$$S_{\text{avp}}^s = 1067.5 - 811.67\delta + 183.59\delta^2, R = 0.997. \quad (8)$$

At a distance of 20 mm from the insert surface, the relationship is as follows:

$$S_{\text{avg}}^{20} = 2048.7 - 1899.2\delta + 474.47\delta^2, R = 0.952. \quad (9)$$

Analysis of Eqs. (8) and (9) shows that the minimum average pearlite grain area near the surface of the inserts reaches $170.4 \mu\text{m}^2$ at an insert thickness of 2.2 mm, and $148.2 \mu\text{m}^2$ at a distance of 20 mm at an insert thickness of 2.0 mm, which is 6 and 14 times smaller, respectively, compared to castings without inserts.

As the study has shown, at gap lengths (Δ , %) within the range of 62–72%, an increase in the solidification rate promotes the formation of a fine-dispersed pearlitic structure.

With further increase in the number of gaps, the intensity of this effect decreases.

The regularity of the influence on the microstructure near the surface of the inserts is described by the following relationship:

$$S_{\text{avp}}^s = 826.01 - 16.848\Delta + 0.1168\Delta^2, R = 0.959. \quad (10)$$

At a distance of 20 mm from the insert surface, the relationship is as follows:

$$S_{\text{avp}}^{20} = 1438.9 - 38.521\Delta + 0.3118\Delta^2, R = 0.775. \quad (11)$$

The analysis results indicate that the most effective influence of reinforcing inserts on the dispersion of the pearlite structure is observed at insert thicknesses ranging from 2.0 to 2.2 mm and a gap length at the 'insert–matrix' interface ranging from 62 to 72%.

4. CONCLUSION

It was established that, during the reinforcement of steel castings with inserts, diffusion bonding zones and defects in the form of gaps are formed at the ‘reinforcing element–matrix’ interface.

An analytical relationship was determined between the length of the gap in the contact zone and the thickness of the inserts.

It was shown that the effect of insert thickness on gap development results from the combined action of two opposing factors: the solidification rate and the heating temperature of the inserts.

Through microstructural analysis of the castings, quantitative parameters of pearlite grain area and their distribution were determined.

Analytical models were developed to describe the influence of insert thickness and gap length on the pearlite grain area in the microstructure of the casting near the insert surface and at a distance of 20 mm from it.

Analysis of the analytical models showed that the most effective influence of reinforcing inserts on pearlite structure refinement is observed at insert thicknesses of 2.0–2.2 mm and gap lengths at the ‘insert–matrix’ interface of 62–72%.

Calculation results indicate that under optimal reinforcement conditions, refinement of the pearlite structure by a factor of 6 to 14 is achievable.

The research was carried out within the framework of Project No. 2023.04/0029 (state registration No. 0124U003980) with the support of a grant from the National Research Foundation of Ukraine under the program ‘Science for Strengthening the Defence Capability of Ukraine’.

AUTHORS’ CONTRIBUTIONS

Y. G. Aftandiliants conceived and designed the research, supervised the project, analysed and interpreted the results, and coordinated the preparation of the manuscript. V. A. Sliusarev contributed to the development of the experimental methodology, participated in the analysis of solidification processes, and assisted in data interpretation. Y. H. Kvasnyts’ka performed microstructural investigations, image analysis, and quantitative evaluation of pearlite grain parameters. I. A. Shalevs’ka participated in theoretical analysis, development of analytical models, and discussion of the mechanisms of reinforcement and gap formation. P. B. Kaliuzhnyi contributed to statistical processing of experimental data, regression analysis, and visualization of results. V. I. Veis carried out experimental casting trials, sample preparation, and metallographic examinations. T. V. Stepanova assisted in literature review, interpretation of results, and manuscript editing.

Z. V. Parkhomchuk contributed to experimental support, data verification, translation and critical revision of the manuscript.

REFERENCES

1. V. A. Efimov and A. S. Eldarkhanov, *Tekhnologii Sovremennoi Metallurgii* [Technologies of Modern Metallurgy] (Moskva: Novyye Tekhnologii: 2004), p. 784 (in Russian).
2. A. A. Shmykov, *Spravochnik Termista* [Heat Treater's Handbook] (Mashgiz: 1956), p. 332 (in Russian).
3. N. I. Nikitenko, V. M. Parshin, and S. D. Postil, *Kristallizatsiya Nepreryvnogo Slitka pri Nalichii Kholodilnika* [Crystallization of a Continuous Casting in the Presence of a Cooler]. In: *Sovershenstvovanie Protsesov Nepreryvnoy Razlivki Stali* (IFTI AN USSR: 1985), p. 203 (in Russian).
4. F. M. Kotlyarskii, *Protsesty Litya*, **3**: 79 (1991).
5. D. M. Belenky and A. G. Vernidub, *Protsesty Litya*, **2**: 28 (1992).
6. O. V. Nosochenko, A. G. Bogachenko, and A. S. Pliskalovskiy, *Povyshenie Kachestva Stal'nykh Slitkov* [Improvement of Steel Ingot Quality] (IFTI AN USSR: 1988), p. 89 (in Russian).
7. V. A. Efimov, G. A. Anisovich, and V. N. Babich, *Spetsial'nyye Sposoby Litya: Spravochnik* [Special Casting Methods: Handbook] (Moskva: Mashinostroenie: 1991), p. 436 (in Russian).
8. L. A. Dan, *Vestnik Priazovskogo Gosudarstvennogo Tekhnicheskogo Universiteta*, **8**: 41 (1999).
9. P. Kaliuzhnyi, I. Shalevska, and V. Sliusarev, *Archives of Metallurgy and Materials*, **68**: 1369 (2023).
10. E. L. Shvedkov, *Ehlementarnaya Matematicheskaya Statistika v Ehksperimental'nykh Zadachakh Materialovedeniya* [Elementary Mathematical Statistics in Experimental Tasks of Materials Science] (Kiev: Naukova Dumka: 1975), p. 111 (in Russian).
11. B. B. Gulyayev, *Teoriya Liteinykh Protsesov* [Theory of Casting Processes] (Moskva: Mashinostroenie: 1976), p. 216 (in Russian).